

## SUPPLEMENTARY MATERIAL

### Exploring quantum tunneling in heavy atom reactions using a rigorous theoretical approach to the dynamics. Formation of NO + O from the N + O<sub>2</sub> atmospheric reaction

Fabrizio Esposito,<sup>a</sup> Pablo Gamallo,<sup>b</sup> Miguel González,<sup>b,\*</sup> and Carlo Petrongolo

<sup>a</sup>Istituto per la Scienza e Tecnologia dei Plasmi, Consiglio Nazionale delle Ricerche, Sede Territoriale di Bari, Via Amendola 122/D, 70126 Bari, Italy

<sup>b</sup>Departament de Ciència de Materials i Química Física and Institut de Química Teòrica i Computacional (IQTC), Universitat de Barcelona, Martí i Franquès 1-11, 08028 Barcelona, Spain

<sup>c</sup>Istituto per i Processi Chimico Fisici, Consiglio Nazionale delle Ricerche, Via G. Moruzzi 1, 56124 Pisa, Italy

#### Contents

These contents mainly present additional figures on the reaction probability.

- <b>ZPE issue and N+O<sub>2</sub> reaction</b>	p. 2
- <b>Figure S1.</b> Comparison of histogram and Gaussian binning in the QCT reaction probability for $J=0$	p. 3
- <b>Figure S2.</b> QM and QCT reaction probabilities multiplied by the $(2J+1)$ term vs. $J$ , for a selection of $E_{\text{col}}$ values.	p. 4
- <b>Figure S3.</b> QM and QCT reaction probabilities as a function of $E_{\text{col}}$ , for a selection of $J$ values.	p. 5
- <b>Figure S4.</b> QM reaction probability as a function of $E_{\text{col}}$ , for a selection of $J$ values in the 0-90 interval and considering $p=+$ and $K_0=0$ .	p. 6
- <b>Figure S5.</b> Effective potential energy as a function of $R$ , for $J=50$ and considering $K_0=0$ and 1.	p. 6
- <b>Figure S6.</b> QM reaction probability as a function of $E_{\text{col}}$ , for a selection of $J$ values in the 0-30 interval and considering $K_0=0$ and $K_0=1$ .	p. 7
- <b>Figure S7.</b> QM reaction probability as a function of $E_{\text{col}}$ , for $J=0$ and considering $j_0$ values in the 1-17 interval.	p. 7
- <b>Figure S8.</b> QM and QCT reaction cross sections. Comparison with previous QM approximate results.	p. 8
- <b>Figure S9.</b> QM and QCT rate constants for N + O <sub>2</sub> ( $v_0=0, j_0=1$ ) and experimental thermal rate constant for N + O <sub>2</sub> .	p. 8
- <b>References</b>	p. 9

## Zero point energy issue and N+O<sub>2</sub> reaction

There are two cases in which the zero point energy (ZPE) effect can be relevant in QCT. The first and most important one is related to polyatomic molecules, in which more than one vibrational degree of freedom is present. As a consequence, it is very likely that the initial vibrational energy of one vibrational mode leaks into the others, even before the interaction with the target takes place (ref. S1). The second case is in the presence of an endothermic reaction, when the product can be formed classically with a final distribution systematically lower than the ZPE. In this condition, the product lowest vibrational bin is covered by a strongly uneven distribution, which gives origin to inaccuracies (refs. S2 and S3). This condition is present when the barrier to reaction is lower than the product ZPE, and the total energy is just sufficient for reaction by overcoming the barrier (of course excluding tunneling in classical dynamics). This issue can be seen as part of a more general problem of final analysis by binning in QCT, when the final distribution does not span the whole width of a bin (refs. S2 and S3). On the contrary, when total energy is higher than final ZPE, the final vibrational action tends to be smoothly distributed at least on the lowest vibrational bin, with good accuracy.

In this work, we consider the products without a final state analysis. Using a standard histogram binning (HB) and then summing final products is exactly equivalent to avoid any final state analysis. If a Gaussian binning is used, however, the result can differ, because it depends on the final distribution in each bin. In the present conditions (exothermicity much higher than product ZPE, presence of a deep well in the strong coupling region), the strong interaction in the A+BC collision tends to give origin to wide product distributions, which will not produce significantly different results when using different binning schemes. A result using GB is presented in Figure S1, where the reaction probability at  $J=0$  is shown, as calculated using histogram binning and Gaussian binning from the same set of trajectories used in this study. The two results differ only for larger statistical fluctuations associated with GB, as expected, because many trajectories are discarded using this procedure. No significant difference is observed concerning reaction threshold.

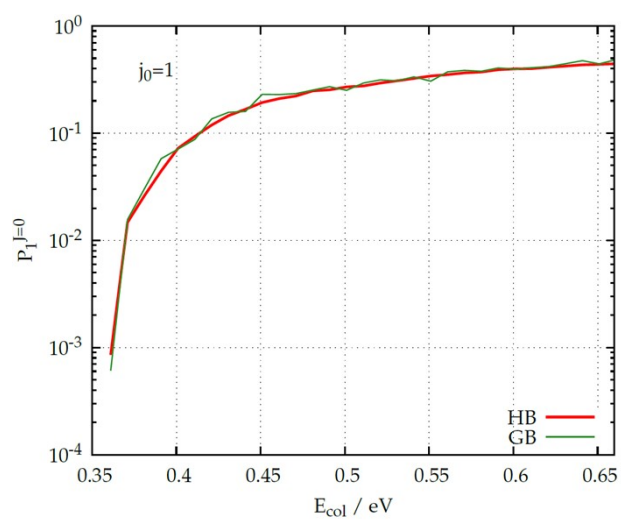


**Figure S1.** Comparison of histogram binning (HB) and Gaussian binning (GB) applied to the QCT reaction probability calculation for  $J=0$ , including the set of trajectories used in this work. The two results differ only for slightly worse statistics associated with GB.

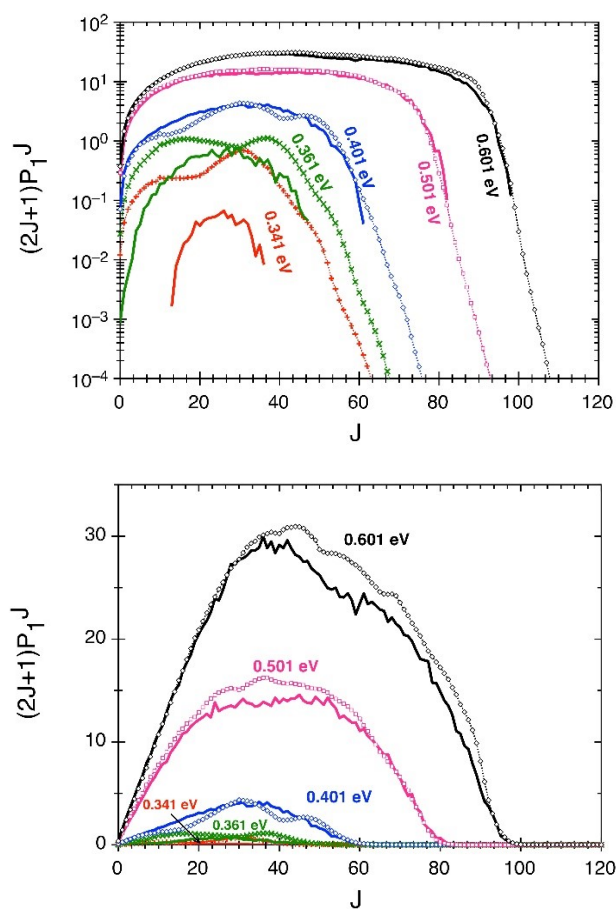


**Figure S2.** QM (symbols) and QCT (lines) reaction probabilities multiplied by the  $(2J+1)$  term as a function of  $J$ , for a selection of  $E_{\text{col}}$  values. This figure complements Figure 1.

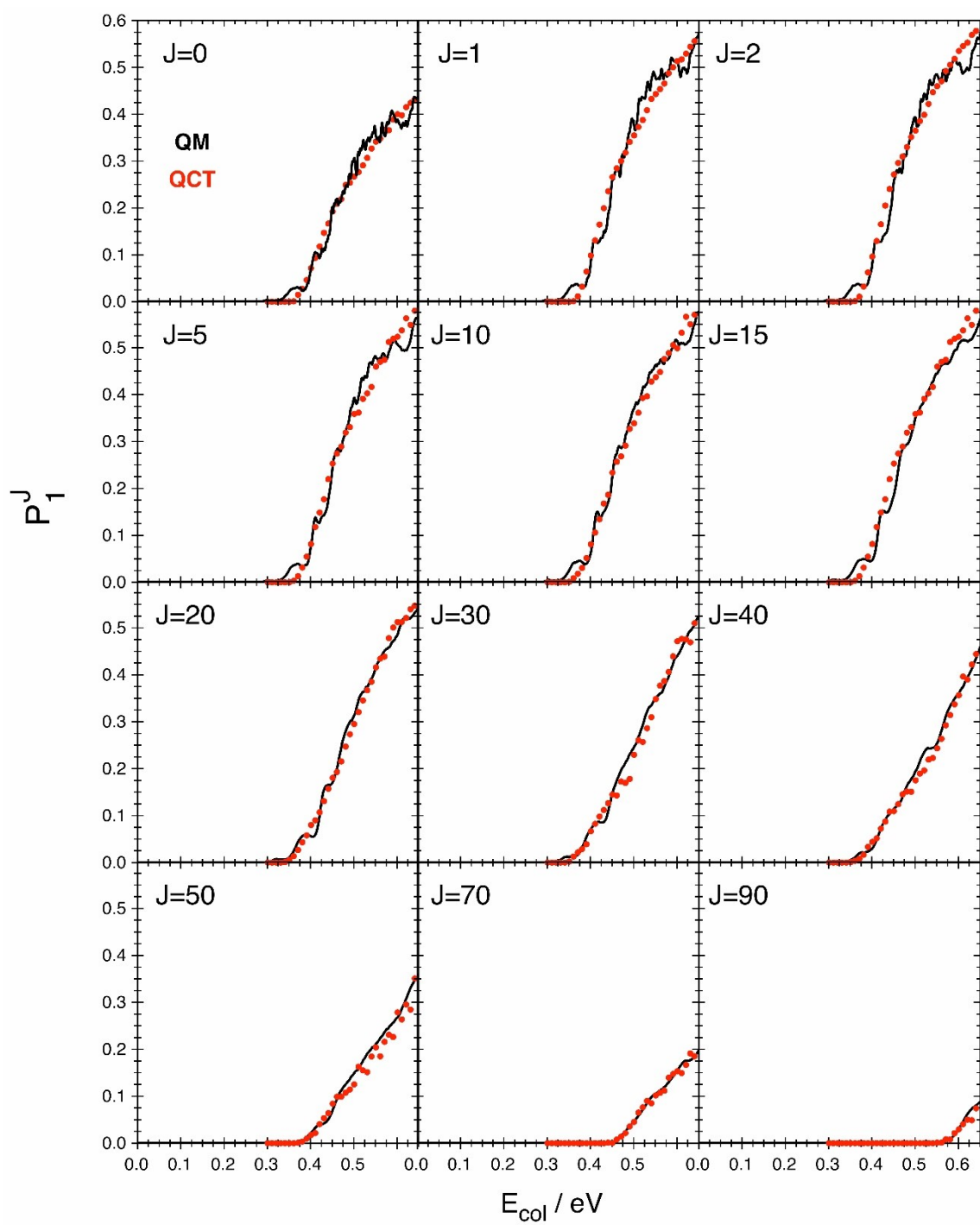


**Figure S3.** QM (black) and QCT (red) reaction probabilities as a function of  $E_{\text{col}}$ , for a selection of  $J$  values.

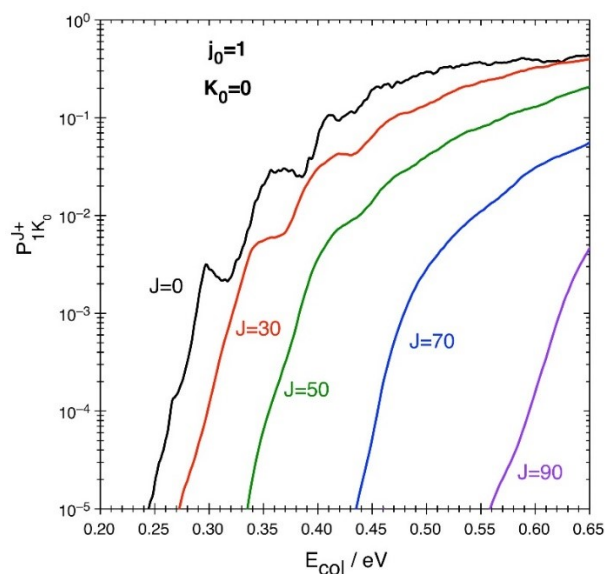


**Figure S4.** QM reaction probability as a function of  $E_{col}$ , for a selection of  $J$  values in the 0-90 interval and considering  $p=+$  and  $K_0=0$ .

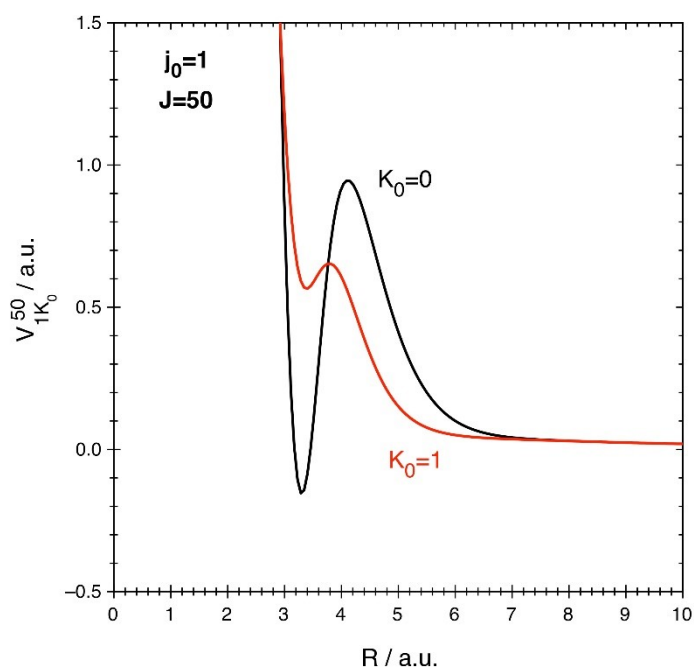


**Figure S5.** Effective potential energy as a function of  $R$ , for  $J=50$  and considering  $K_0=0$  and 1. This potential energy is defined as

$$V_{jK}^J(R) = \min_{r,\gamma} V(R,r,\gamma) + \frac{[J(J+1) + j(j+1) - 2K^2]}{2\mu_R R^2}$$

where the different symbols have the usual meaning.<sup>S4</sup> In this expression the potential energy (PES) is minimized with respect to  $r$  and  $\gamma$ .

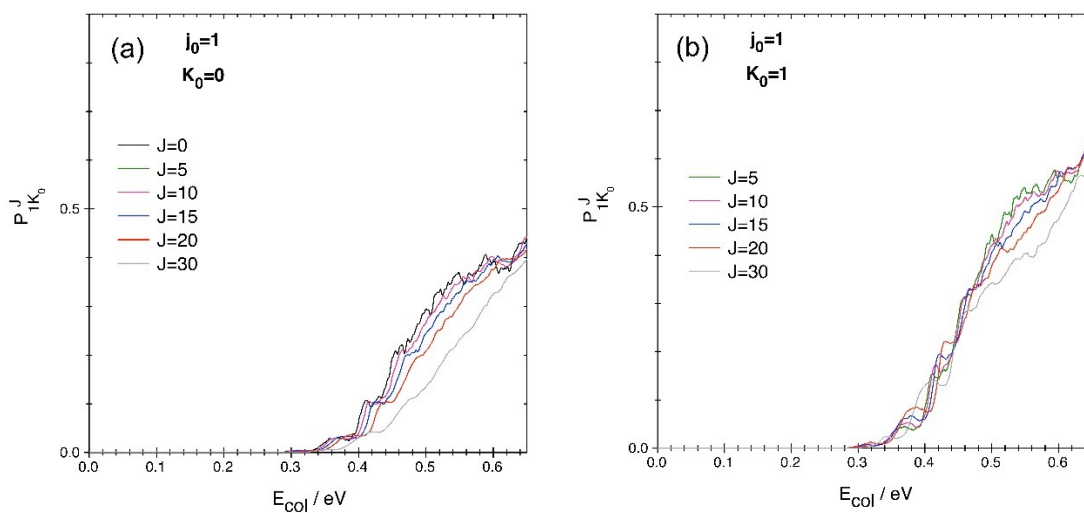


**Figure S6.** QM reaction probability as a function of  $E_{\text{col}}$ , for a selection of  $J$  values in the 0-30 interval and considering  $K_0=0$  (a) and  $K_0=1$  (b).

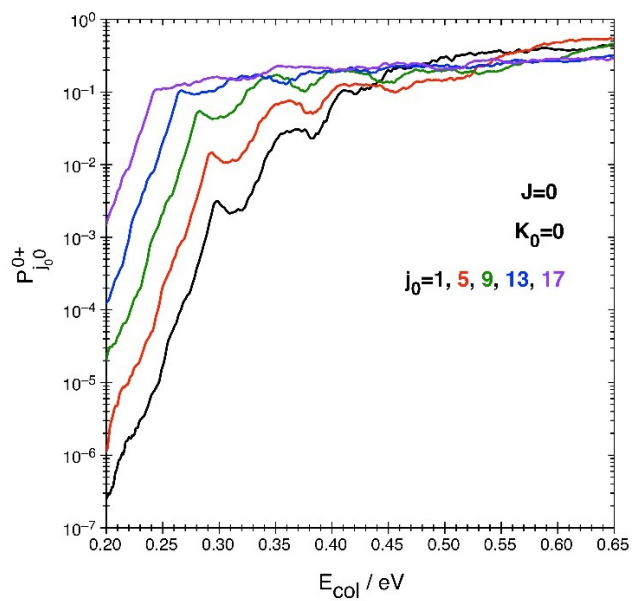


**Figure S7.** QM reaction probability as a function of  $E_{\text{col}}$ , for  $J=0$  and considering  $j_0$  values in the 1-17 interval.

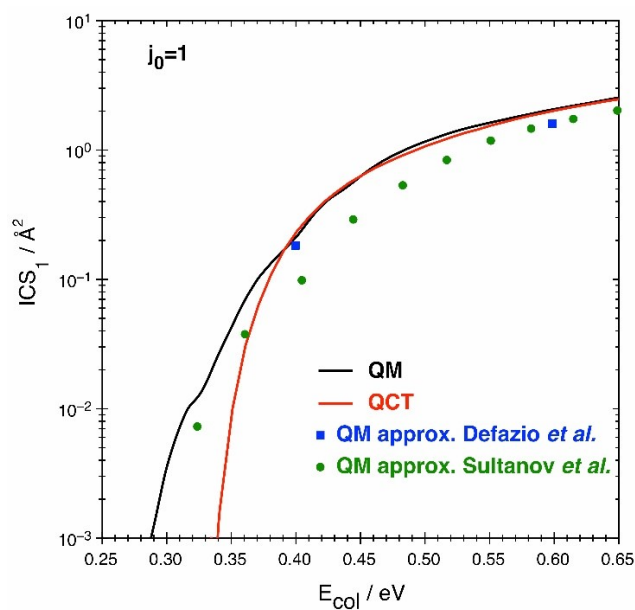


**Figure S8.** Comparison of the QM and QCT cross sections obtained here with the QM approximate ones ( $J$ -shifting approximation) reported by Defazio et al. (time dependent QM (RWP))<sup>S5</sup> and Sultanov and Balakrishna (time independent QM).<sup>S6</sup>

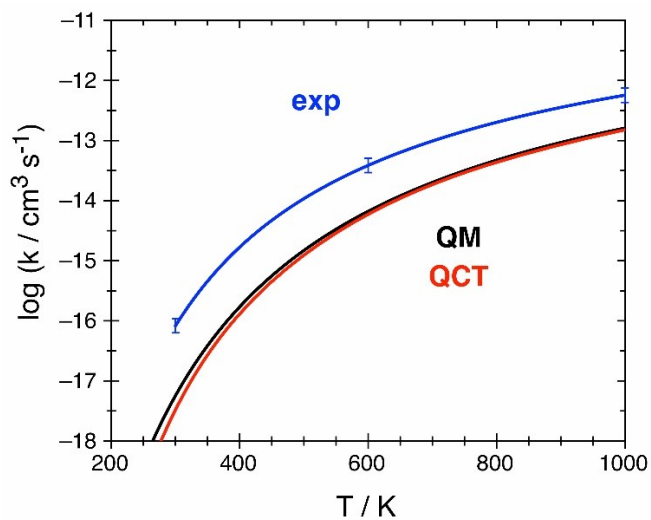


**Figure S9.** QM (black) and QCT (red) rate constants for  $\text{N} + \text{O}_2(v_0=0, j_0=1) \rightarrow \text{NO} + \text{O}$  and experimental (blue) thermal rate constant for  $\text{N} + \text{O}_2 \rightarrow \text{NO} + \text{O}$  including error bars.<sup>S7</sup>

## References

- <sup>S1</sup> G. Czako, A. L. Kaledin, J. M. Bowman, "A practical method to avoid zero-point leak in molecular dynamics calculations: application to the water dimer", *J. Chem. Phys.* **132**, 164103 (2010).
- <sup>S2</sup> F. Esposito, "Reactivity, relaxation and dissociation of vibrationally excited molecules in low-temperature plasma modeling", *Rend. Lincei-Sci. Fis.* **30**, 57-66 (2019).
- <sup>S3</sup> F. Esposito, R. Macdonald, I. D. Boyd, K. Neitzel and D. A. Andrienko, "Heavy-particle elementary processes in hypersonic flows", in "Hypersonic meteoroid entry physics", edited by G. Colonna, M. Capitelli and A. Laricchiuta, IOP Publishing, Bristol (2019), pp 16-1 to 16-32.
- <sup>S4</sup> P. Gamallo, M. González, R. Sayós and C. Petrongolo, "Quantum wave packet dynamics of the  $1^3A'' N(^4S) + NO(\tilde{X}^2\Pi) \rightarrow N_2(\tilde{X}^1S_g^+) + O(^3P)$  reaction", *J. Chem. Phys.* **119**, 7156-7162 (2003).
- <sup>S5</sup> P. Defazio, C. Petrongolo, C. Oliva, M. González, and R. Sayós, "Quantum dynamics of the  $N(^4S) + O_2$  reaction on the  $X^2A'$  and  $a^4A'$  surfaces: reaction probabilities, cross sections, rate constants, and product distributions", *J. Chem. Phys.* **117**, 3647-3655 (2002).
- <sup>S6</sup> R. A. Sultanov and N. Balakrishnan, "Quantum mechanical investigations of the  $N(^4S) + O_2(X^3\Sigma_g^-) \rightarrow NO(X^2\Pi) + O(^3P)$  reaction", *J. Chem. Phys.* **124**, 124321 (2006).
- <sup>S7</sup> D. L. Baulch, C. J. Cobos, R. A. Cox, G. Hayman, Th. Just, J. A. Kerr, T. Murrells, M. J. Pilling, J. Troe, R. W. Walker and J. Warnatz, Evaluated kinetic data for combustion modelling, Supplement I. *J. Phys. Chem. Ref. Data* **23**, 847 (1994) and references cited therein.